



Repositorio Institucional de la Universidad Autónoma de Madrid

<https://repositorio.uam.es>

Esta es la **versión de autor** del artículo publicado en:
This is an **author produced version** of a paper published in:

Journal of Materials Chemistry C 3.5 (2015): 985-989

DOI: <http://dx.doi.org/10.1039/c4tc02662d>

Copyright: © The Royal Society of Chemistry 2015.

El acceso a la versión del editor puede requerir la suscripción del recurso
Access to the published version may require subscription

A Columnar Liquid Crystal with Permanent Polar Order

J. Guilleme,^a J. Aragón,^b E. Ortí,^b E. Cavero,^c T. Sierra,^{c,*} J. Ortega,^d C. L. Folcia,^e J. Etxebarria,^{e,*} D. González-Rodríguez^{a,*} and Tomás Torres^{a,*}

The self-assembly of axial dipolar subphthalocyanine molecules in the presence of electric fields leads to uniaxially oriented columnar liquid crystalline materials that exhibit permanent polarization.

Columnar liquid crystals (LCs) made of discotic π -conjugated semiconductors offer a combination of attributes that are very appealing in several optoelectronic technologies.¹ Their propensity to form stable columns by intermolecular π - π interactions and their fluid nature allows for their organization into oriented materials by means of diverse techniques.² Among them, the use of electric fields arise as particularly useful³ since 1) it can control homeotropic column alignment in defined areas between patterned electrodes,⁴ and 2) it may lead to the generation of thin films that exhibit net polarization.⁵ The latter is viewed as a property of great potential for those applications that require an efficient directional transport of charge carriers,⁶ such as field-effect transistors and photovoltaics, where the design of high dielectric layers and polar electronic interfaces is gaining importance.⁷

In order to produce columnar LC materials that exhibit macroscopic polarization a non-centrosymmetric organization is required,⁸ and for such goal several strategies have been practiced.³ One of them is the use of molecules with dipoles that are parallel to the column axis, either by the stacking of bowl-shaped structures,^{5a,9} or by the incorporation of dipolar amide or urea groups.^{4b,e,5,10} Spontaneous polarization in LC materials typically relies on temporal conformational or orientational arrangements of dipoles and is quite sensitive in practice to external conditions such as cell surfaces or applied field, which is valuable for ferroelectric switching applications.^{3,9d} However, for the same reason, the realization of columnar LC materials with permanent polarization, that persists even in the presence of electric fields of opposite sense, remains a challenging task. Polar order in the columnar materials developed so far is eventually lost with time due to structural relaxation processes that lead to dipole readjustments.

Here we study columnar LC films that can be efficiently aligned parallel to an electric field and that maintain their polar order upon electric field suspension or even inversion. Our strategy relies on the use of conformationally rigid (i.e. non-invertible),¹¹ bowl-shaped mesogens with a strong axial dipole moment, like the C_3 -symmetric boron subphthalocyanine (SubPc)^{12,13} **1** (Figure 1). The key to generate a head-to-tail non-centrosymmetric columnar stacking^{14,15} with a strong axial dipole was the introduction of a small, highly electronegative atom linked to the central boron, such as fluorine.

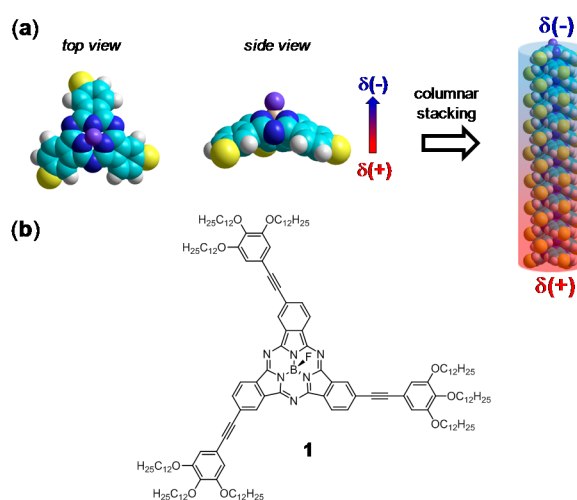


Figure 1. (a) Top and side views of the axial dipolar SubPcBF macrocycle. The yellow spheres represent the arylethynyl substituents. Head-to-tail stacking leads to polarized columnar structures. (b) Structure of the C_3 -symmetric SubPc **1**.^{16,17}

The thermal properties of **1** were studied by polarized optical microscopy (POM) and differential scanning calorimetry (DSC). SubPc **1** displays pseudo focal-conic textures between crossed polarizers, which are characteristic of a hexagonal columnar mesophase (Figure 2a).^{4b,5a,9b,c,10a} According to DSC thermograms (Figure S2), **1** is crystalline as synthesized but, once melted to the isotropic liquid (I), the mesophase appears on cooling at 89.2 °C, and maintains stable at room temperature for several weeks. During the second heating process the Col_h mesophase undergoes a cold crystallization, with no texture change, and this crystal melts into the I phase at 101.2 °C. Subsequent cooling-heating cycles show the same type of thermogram.

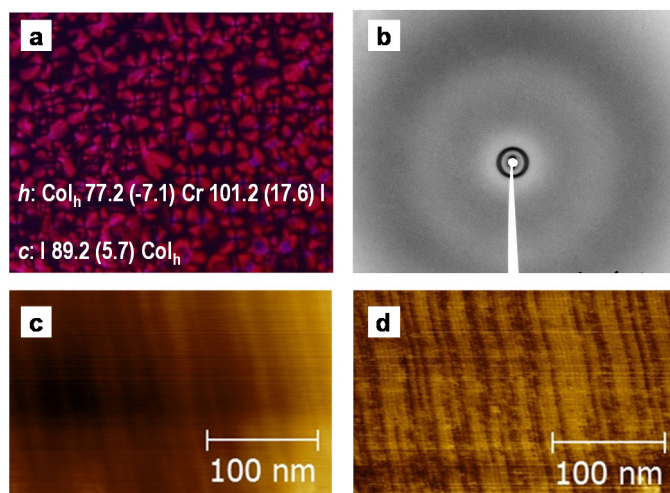


Figure 2. (a) POM photograph (x50) taken at r.t. on cooling from the I phase. Transition temperatures (°C) and enthalpy values (kJ/mol) correspond to the second heating (h)-cooling (c) cycle recorded at 10 °C/min. (b) X-ray diffractogram taken at r.t. on a thermally treated sample (c) AFM topography and (d) 2D phase images of a thermally treated sample of **1** deposited onto mica.

The mesophase arrangement of **1** was studied by X-ray diffraction (XRD) at room temperature. Experiments performed on samples previously heated up to the isotropic liquid, and cooled down at a rate of ca. 10 °C/min, yielded an intense maximum at the low-angle region and a broad diffuse maximum in the wide-angle region (Figure 2b). The low-angle peak can be related with the (10) reflection of a hexagonal columnar phase. The absence of higher order reflections¹⁸ makes it difficult to unambiguously assign the mesophase type exclusively by XRD. Nevertheless, according to POM observations, we propose that the small-angle maximum corresponds to the (10) reflection of a hexagonal arrangement with a cell parameter (a) of 39.0 Å. Additionally, AFM tapping mode images, taken at r.t. to a thermally treated sample (*vide supra*) of **1** on mica, show line patterns that are consistent with different domains of columns arranged onto the surface (Figures 2c-d and S3). Surface analysis showed a mean periodicity between lines of 40 Å, which is within the range of the distance measured by XRD and attributed to the hexagonal cell parameter. Furthermore, an XRD diagram recorded in the crystalline state (8 weeks after thermal treatment) is consistent with the hexagonal columnar arrangement (see Figure S4 and Table S1). Finally, the diffuse maximum at wide angles, typically observed in all kind of mesophases, is unusually broad in this case (Figures 2b and S5). Part of the contribution to that reflection can be attributed to the liquid-like order of the hydrocarbon chains (distances around 4.5 Å), but the reflection further extends at higher angles, covering distances down to 2.5 Å. These small spacings should correspond to intracolumnar distances.

To gain more insight into the structure of the **1** assemblies in the mesophase, semiempirical quantum-chemical calculations were carried out.¹⁷ A hexagonal columnar model, formed by 7 columns and 4 molecules per column, was built up and, subsequently, its structure was fully relaxed at the PM7 level (see Figures S7 and S8). The average distance between the stacking axes of the **1** columns is computed at 42.2 Å, in good agreement with the lattice parameter (39.0 Å) derived from XRD data and the mean periodicity (40 Å) measured in AFM images. Calculations also indicate that aggregation within a column is not

only dominated by dispersion or van der Waals forces, but also by strong $F^{\delta-}\cdots B^{\delta+}$ dipolar interactions between adjacent SubPcs.^{17,19}

We were interested in studying the evolution of the axial dipole moment with the size of the system. Stacks of increasing length, comprising 1, 4, 8, 12, 16 and 20 molecules, were computed using a column extracted from the PM7-optimized hexagonal lattice as a building block. Our results indicate that the dipole moment follows the stacking axis and systematically increases from 13.7 D for the **1** monomer to 281.6 D in a columnar icosamer (see Figure S9). Additionally, the influence of an electric field (12 V/μm) on the energy of the dipolar stacks was evaluated at the PM7 level (Figure S9). A slight stabilization/destabilization of the columnar aggregate is seen when such field is applied parallel/antiparallel to the polarization vector. The energy difference between parallel and antiparallel arrangements increases linearly with the stack size reaching 3.2 kcal/mol in the icosamer.

The Col_h mesophase of **1** was next studied in commercial Linkam cells, comprised of two ITO plates separated by 5 μm, in order to investigate electric field columnar alignment. The material in the cell was cooled from the isotropic liquid into the Col_h mesophase while applying a triangular-wave AC voltage (90 V_{pp}, 0.08 Hz). In this cooling process, the ITO area appeared non-birefringent between crossed-polarizers, whereas a birefringent texture became visible in the area without electrodes (Figure 3a). The absence of birefringence under field indicates a uniaxial character of the mesophase thus reinforcing the hexagonal symmetry assigned to the mesophase structure.^{4,9} On heating the sample, this black texture persists up to the transition to the isotropic liquid at 101.2 °C, which is clearly observed in the birefringent areas without electrodes. Repeating the cooling process without electric field led on the other hand to the development of a birefringent texture on the full cell area. Once the material reaches the mesophase on cooling, the dark area between electrodes does not show up with applied AC voltage. These observations suggest that the marked dipole moment of the mesogens, perpendicular to the SubPc core, prompt them to interact with the electric field during the I-Col_h transition. Accordingly, unidirectional orientation of the columns along the electric field is achieved, and remains stable in the mesophase once the electric field is turned off.

We then investigated the LC material in the Linkam cells described above using second harmonic generation (SHG), which is a convenient and reliable method to determine the existence of polarity in the presence and absence of an electric field. A setup²⁰ including a Nd:YAG laser with a fundamental wavelength $\lambda = 1064$ nm was used. SHG signal is observed in the mesophase when the material is cooled down from the isotropic liquid under a DC field. The SHG response is preserved after turning off the field. The SHG light is π polarized, regardless of whether the fundamental light is π or σ (Figure 3b). In addition, the SHG signal is null at normal incidence (Figure 3c). These characteristics indicate that the material has a macroscopic polar axis along the field direction, with a susceptibility tensor of the same symmetry than poled polymers.¹⁷ The induced polar axis is thermally stable and is kept up to the clearing point (Figure 3d). Remarkably, the SHG signal is maintained at room temperature for several weeks without appreciable degradation.

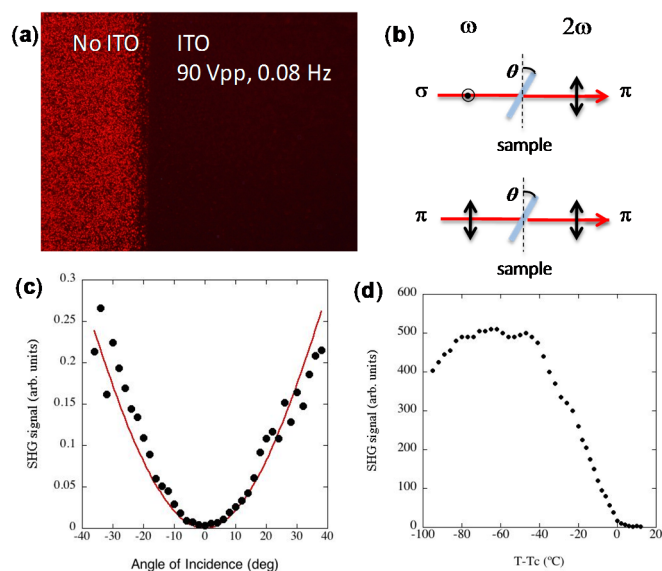


Figure 3. (a) POM photograph ($\times 20$; r.t.) of a $5 \mu\text{m}$ sandwich cell with ITO electrodes. An electric field was applied during the I-Col_h transition that provoked the orientation of the columns. (b) Schematic illustration showing the SHG light polarization for different polarizations of the fundamental wave. (c) SHG signal at $40 \text{ }^\circ\text{C}$ as a function of the angle of incidence for the $\sigma \rightarrow \pi$ conversion. The solid line is a theoretical fit giving $d_{31} = 0.5 \text{ pm/V}$. (d) Temperature dependence of the SHG signal at an angle of incidence of 30° . The origin is the clearing point (T_c).

We used SHG interferometry to analyze the switching behavior of the **1** material. The setup (Figure 4a) is designed to permit the interference of the SHG signals from the sample and a quartz plate. A relative phase shift between the two SHG waves is produced as a consequence of the optical path difference between the fundamental and SHG waves in the glass plate. The phase shift is controlled by rotating the glass plate, and the resulting SHG signal shows interference fringes as the rotation angle is varied. When the LC sample is obtained from the isotropic liquid under opposite DC fields interference patterns in antiphase are attained (blue and red points in Figure 4b). In addition, the pattern remains unaltered if the field is turned off or even reversed within the mesophase range (black dots in Figure 4b). This indicates that the liquid crystal sample is permanently polarized once formed, but it is not electrically invertible. In other words, the mesophase is not ferroelectric but pyroelectric. The directional sense of the macroscopic polarization can only be reversed by heating the material up to the isotropic phase and cooling down again under an opposite field. A schematic illustration of the polarization behavior under electric field and temperature treatment is shown in Figure 5.

It is interesting to have an idea of the degree of polar order in the structure. To evaluate this parameter, the magnitude of the SHG signal was analyzed. By comparing an estimate of the microscopic molecular hyperpolarizabilities²¹ with the macroscopic SHG signal, a minimum threshold for polar order in the mesophase of 35 % was deduced¹⁷ for an applied electric field of $12 \text{ V}/\mu\text{m}$ in the I phase. This degree of order corresponds to a remnant polarization of $400 \text{ nC}/\text{cm}^2$ (taking the dipole moment of 13.7 D derived from our PM7 calculations). Larger electric fields induce higher order, but fields above $15 \text{ V}/\mu\text{m}$ are likely to produce dielectric breakdown.

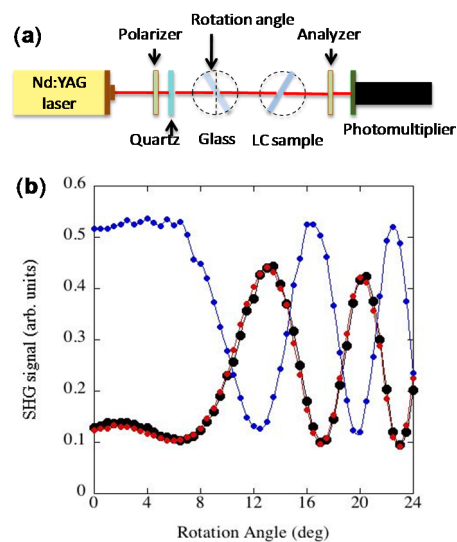


Figure 4. (a) Scheme of the optical setup used for SHG interferometry. The interferograms are obtained by rotating the glass plate. (b) SHG interference patterns at $40 \text{ }^\circ\text{C}$ obtained by rotating the glass plate. Blue and red points correspond to a LC sample that was polarized with (+) and (-) DC electric field respectively, on cooling from the I phase. Black points were obtained by reversing the (-) DC field without heating the sample to the I phase.

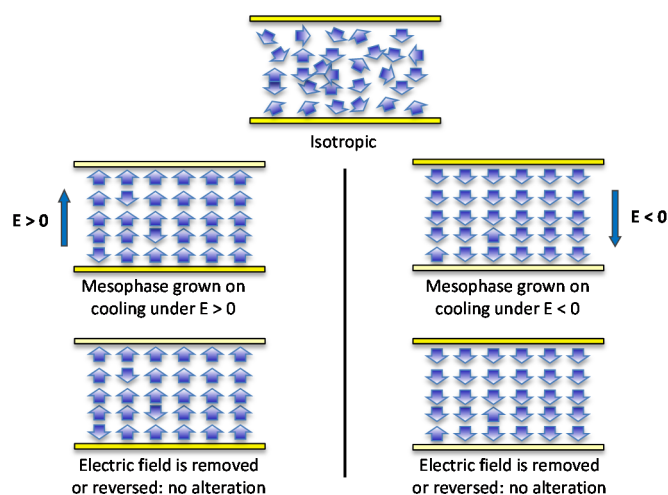


Figure 5. Schematic representation of the polarization behavior of a LC film of **1**. Arrows represent groups of molecular dipoles which assemble in columns in the mesophase. The polarization is developed on cooling the material from the isotropic liquid under a DC electric field. Within the mesophase, the polar order remains unaltered after the electric field is switched off and cannot be reversed.

Conclusions

In conclusion, we have studied a columnar liquid crystal that exhibits permanent polar order along the columnar axis. The polarization orientation is developed under electric field application only when cooling the sample from the isotropic phase. The degree of polar order is large - enough for device applications -,¹³ not sensitive to electric fields of opposite sense, and can be conserved for weeks in the mesophase after the electric field is switched off. This unique effect is ascribed to the

rigidity of our axial dipolar SubPc stacks and differs from related LCs where polar order can eventually vanish or switch due to conformational or orientational changes.

Notes and references

^a Departamento de Química Orgánica, Universidad Autónoma de Madrid, 28049 Madrid, Spain.

^b Instituto de Ciencia Molecular, Universidad de Valencia, 46980 Paterna (Valencia), Spain.

^c Departamento de Química Orgánica, Facultad de Ciencias – Instituto de Ciencia de Materiales de Aragón (ICMA), CSIC – Universidad de Zaragoza, 50009 Zaragoza, Spain.

^d Departamento de Física Aplicada II; Facultad de Ciencia y Tecnología, UPV/EHU, 48080, Bilbao, Spain.

^e Departamento de Física de la Materia Condensada, Facultad de Ciencia y Tecnología, UPV/EHU, 48080, Bilbao, Spain.

Funding from MINECO (MAT2012-38538-CO3-01, 02 and CTQ2012-31914), MICINN and MEC (F.P.U. fellowship (JG)), CTQ-2011-24187/BQU, CTQ2011-23659 and Consolider-Ingenio Nanociencia Molecular, CDS2007-00010), Comunidad de Madrid (MADRISOLAR-2, S2009/PPQ/1533), European Research Council (StG-279548), Aragon government, E04, Basque Country Government GI/IT-449-10, Generalitat Valenciana (PROMETEO/ 2012/053), and FEDER is acknowledged. We thank the Advanced Microscopy Laboratory (LMA) for the AFM studies.

Electronic Supplementary Information (ESI) available: Experimental details and additional characterization data. Figures S1-S9. See DOI: 10.1039/c000000x/

- For recent reviews on columnar liquid crystals see: a) S. Sergeev, W. Pisula, Y. H. Geerts, *Chem. Soc. Rev.*, **2007**, *36*, 1902; b) S. Laschat, A. Baro, N. Steinke, F. Giesselmann, C. Hägele, G. Scalia, R. Judele, E. Kapatsina, S. Sauer, A. Schreivogel, M. Tosoni, *Angew. Chem. Int. Ed.*, **2007**, *46*, 4832; c) B. R. Kaafarani, *Chem. Mater.*, **2011**, *23*, 378.
- (a) M. Yoshio, T. Kagata, K. Hoshino, T. Mukai, H. Ohno, T. Kato, *J. Am. Chem. Soc.* **2006**, *128*, 5570; b) H. Monobe, K. Awazu, Y. Shimizu, *Adv. Mater.* **2006**, *18*, 607; c) R. I. Gearba, D. V. Anokhin, A. I. Bondar, W. Bras, M. Jahr, M. Lehmann, D. A. Ivanov, *Adv. Mater.* **2007**, *19*, 815; d) S. Furumi, K. Ichimura, *Phys. Chem. Chem. Phys.* **2011**, *13*, 4919.
- a) H. Takezoe, K. Kishikawa, E. Gorecka, *J. Mater. Chem.* **2006**, *16*, 2412; b) S. Horiuchi, Y. Tokura, *Nature Mater.* **2008**, *7*, 357; c) H. Takezoe, F. Araoka, *Liq. Cryst.* **2013**, *41*, 393.
- a) H. Shimura, M. Yoshio, A. Hamasaki, T. Mukai, H. Ohno, T. Kato, *Adv. Mater.* **2009**, *21*, 1591; b) D. Miyajima, F. Araoka, H. Takezoe, J. Kim, K. Kato, M. Takata, T. Aida, *Angew. Chem. Int. Ed.* **2011**, *50*, 7865; c) M. Yoshio, Y. Shoji, Y. Tochigi, Y. Nishikawa, T. Kato, *J. Am. Chem. Soc.* **2009**, *131*, 6763; d) M. Yoshio, R. Konishi, T. Sakamoto, T. Kato, *New J. Chem.* **2013**, *37*, 143; e) F. Araoka, S. Masuko, A. Kogure, D. Miyajima, T. Aida, H. Takezoe, *Adv. Mater.* **2013**, *25*, 4014; f) N. Hu, R. Shao, Y. Shen, D. Chen, N. A. Clark, D. M. Walba, *Adv. Mater.* **2014**, *26*, 2066.
- a) D. Miyajima, F. Araoka, H. Takezoe, J. Kim, K. Kato, M. Takata, T. Aida, *J. Am. Chem. Soc.* **2010**, *132*, 8530; b) C. F. C. Fitié, W. S. C. Roelofs, M. Kemerink, R. P. Sijbesma, *J. Am. Chem. Soc.* **2010**, *132*, 6892; c) C. F. C. Fitié, W. S. C. Roelofs, P. C. M. Magusin, M. Wübbenhorst, M. Kemerink, R. P. Sijbesma, *J. Phys. Chem. B* **2012**, *116*, 3928.
- T. Amaya, S. Seki, T. Moriuchi, K. Nakamoto, T. Nakata, H. Sakane, A. Saeiki, S. Tagawa, T. Hirao, *J. Am. Chem. Soc.* **2009**, *131*, 408.
- a) P. Paoprasert, B. Park, H. Kim, P. Colavita, R. J. Hamers, P. G. Evans, P. Gopalan, *Adv. Mater.* **2008**, *20*, 4180; b) K. Asadi, P. W. M. Blom, D. M. de Leeuw, *Appl. Phys. Lett.* **2011**, *99*, 053306.
- D. M. Walba, Ferroelectric Liquid Crystals. A Unique State of Matter. in *Advances in the Synthesis and Reactivity of Solids*; T. E. Mallouk, Ed.; JAI Press Ltd.: Greenwich, CT, 1991; Vol. **1**, p 173.
- a) E. Gorecka, D. Pocięcha, J. Mieczkowski, J. Matraszek, D. Guillon, B. Donnio, *J. Am. Chem. Soc.* **2004**, *126*, 15946; b) D. Miyajima, K. Tashiro, F. Araoka, H. Takezoe, J. Kim, K. Kato, M. Takata, T. Aida, *J. Am. Chem. Soc.* **2009**, *131*, 44; c) K. Sato, Y. Itoh, T. Aida, *J. Am. Chem. Soc.* **2011**, *133*, 13767; d) D. Miyajima, F. Araoka, H. Takezoe, J. Kim, K. Kato, M. Takata, T. Aida, *Science*, **2012**, *336*, 209.
- M. L. Bushey, T.-Q. Nguyen, C. Nuckolls, *J. Am. Chem. Soc.* **2003**, *125*, 8264; b) K. Kishikawa, S. Nakahara, Y. Nishikawa, S. Kohmoto, M. Yamamoto, *J. Am. Chem. Soc.* **2005**, *127*, 2565.
- SubPcs are rigid macrocycles that cannot undergo bowl inversion (i.e. racemization). In this sense, they are like triquinacenes, but differ from other bowl-shaped molecules, such as regular cyclotrimertrilene, calixarene, sumanene or corannulene. See ref. 12 and: a) S. Shimizu, A. Miura, S. Khene, T. Nyokong, N. Kobayashi, *J. Am. Chem. Soc.* **2011**, *133*, 17322; b) G. Markopoulos, L. Henneicke, J. Shen, Y. Okamoto, P. G. Jones, H. Hopf, *Angew. Chem. Int. Ed.* **2012**, *51*, 12884.
- a) C. G. Claessens, D. González-Rodríguez, T. Torres, *Chem. Rev.* **2002**, *102*, 835; b) C. G. Claessens, D. González-Rodríguez, M. S. Rodríguez-Morgade, A. Medina, T. Torres, *Chem. Rev.* **2014**, *114*, 2192.
- These magenta 14- π -aromatic dyes have generated significant technological interest in several applied fields. See: a) C. G. Claessens, D. González-Rodríguez, T. Torres, G. Martín, F. Agulló-López, I. Ledoux, J. Zyss, V. R. Ferro, J. M. García de la Vega, *J. Phys. Chem.* **2005**, *109*, 3800; b) D. González-Rodríguez, T. Torres, D. M. Guldi, J. Rivera, M. A. Herranz, L. Echegoyen, *J. Am. Chem. Soc.* **2004**, *126*, 6301; c) D. González-Rodríguez, E. Carbonell, D. M. Guldi, T. Torres, *Angew. Chem. Int. Ed.* **2009**, *48*, 8032; d) G. E. Morse, J. S. Castrucci, M. G. Helander, Z.-H. Lu, T. P. Bender, *ACS Appl. Mater. Interfaces* **2011**, *3*, 3538; e) S. M. Menke, W. A. Luhman, R. J. Holmes, *Nature Mater.* **2012**, *12*, 152; f) B. Verreet, D. Cheyns, P. Heremans, A. Stesmans, G. Zango, C. G. Claessens, T. Torres, B. P. Rand, *Adv. Energy Mater.* **2014**, DOI 10.1002/aenm.201301413.
- The hexagonal columnar head-to-tail stacking of SubPcBF molecules was proven in monocrystalline samples. See: M. S. Rodríguez-Morgade, C. G. Claessens, A. Medina, D. González-Rodríguez, E. Gutierrez-Puebla, A. Monge, I. Alkorta, J. Elguero, T. Torres, *Chem. Eur. J.* **2008**, *14*, 1342.
- Tribenzotriquinanes have been shown to spontaneously pack in polar uniaxial crystalline structures. See: J. G. Brandenburg, S. Grimme, P. G. Jones, G. Markopoulos, H. Hopf, M. K. Cyranski, D. Kuck, D. *Chem. Eur. J.* **2013**, *19*, 9930.
- The synthesis and characterization of racemic, C_3 -symmetric **1** can be found in the S.I.
- See the Supporting Information for further details.

- 18 The absence of the (11) reflection is not infrequent in X-ray patterns of hexagonal columnar mesophases and it is due to a minimum in the form factor, which precludes the observation of peaks at this diffraction angle. See: a) B. Kohne, K. Praefcke, W. Stephan, *Chimia* 1986, **40**, 14; b) H. Strzelecka, C. Jallabert, M. Veber, P. Davidson, A. M. Levelut, *Mol. Cryst. Liq. Cryst.* 1988, **161**, 395; c) J. Barberá, C. Cativiela, J. L. Serrano, M. M. Zurbano, *Adv. Mater.* 1991, **3**, 602; d) J-H. Olivier, F. Camerel, J. Barberá, P. Retailleau, R. Ziessel, *Chem. Eur. J.* 2009, **15**, 8163; e) F. Camerel, G. Ulrich, J. Barberá, R. Ziessel, *Chem. Eur. J.* 2007, **13**, 2189; f) J. Barberá, M. Bardají, J. Jiménez, A. Laguna, M. P. Martínez, L. Oriol, J. L. Serrano, I. Zaragoza, *J. Am. Chem. Soc.* 2005, **127**, 8994; g) W. Pisula, Z. Tomovic, Ch. Simpson, M. Kastler, T. Pakula, K. Mullen, *Chem. Mater.* 2005, **17**, 4296.
- 19 The $F^{\delta-} \cdots B^{\delta+}$ contacts are calculated at 2.92 Å, which is slightly longer than 2 times the covalent B–F bond (1.37 Å) and shorter than the sum of the van der Waals radii of B (1.92 Å) and F (1.47 Å).
- 20 N. Pereda, C. L. Folcia, J. Etxebarria, J. Ortega, M. B. Ros, *Liq. Cryst.*, 1998, **24**, 451.
- 21 G. Rojo, F. Agulló-López, B. del Rey, T. Torres, *J. Appl. Phys.* 1998, **84**, 6507.